

Indirect boundary element method combining extra fundamental solutions for solving exterior acoustic problems with fictitious frequencies

Jia-Wei Lee,¹ Jeng-Tzong Chen,^{2,a)} and Chi-Feng Nien³

¹Department of Civil Engineering, Tamkang University, No.151, Yingzuan Road, Tamsui District, New Taipei City 25137, Taiwan, Republic of China

²Center of Excellence for Ocean Engineering, National Taiwan Ocean University, No. 2, Beining Road, Zhongzheng District, Keelung City 20224, Taiwan, Republic of China

³Department of Harbor and River Engineering, National Taiwan Ocean University, No. 2, Beining Road, Zhongzheng District, Keelung City 20224, Taiwan, Republic of China

(Received 10 December 2018; revised 14 April 2019; accepted 27 April 2019; published online 29 May 2019)

The authors propose an alternative approach to solve the problem of fictitious frequencies. It is different from the mixed potential approach in the indirect method as well as the Burton and Miller approach in the direct boundary element method (BEM). The authors add some fundamental solutions with unknown strength in the solution representation to complete the solution space. From the viewpoint of the adding source, the present idea is similar to the combined Helmholtz interior integral equation formulation (CHIEF) method. The difference between the added source point and null-field point of CHIEF is their role. The former supplies the deficient basis due to the fictitious frequency while the latter provides the extra constraint equation. It can be alternatively found by adding the right unitary vectors of zero singular value. The bordered matrix is invertible for the fictitious frequency if the extra source points do not locate at the failure position. This is the reason why the property is analogous to the CHIEF method in the direct BEM. Therefore, it can fill in the blank area of why there is no CHIEF method in the indirect method. The authors also analytically derive the locations of possible failure source points by using the degenerate kernel.

© 2019 Acoustical Society of America. <https://doi.org/10.1121/1.5108621>

[MRB]

Pages: 3116–3132

I. INTRODUCTION

The boundary element method (BEM) and boundary integral equation method (BIEM) have been employed to solve radiation and scattering problems in acoustics and vibration problems. It is well known that fictitious frequency^{1,2} and spurious eigenvalue³ occur in the exterior and interior problems, respectively. In addition, we use the method of fundamental solutions (MFS) as well as the BEM to solve the two dimensional (2D) exterior Helmholtz problems; it may result in the problem of fictitious frequencies. A theoretical proof of the existence of fictitious frequency in the MFS was first addressed by Chen⁴ thanks to the circulant property for a circular case. Regarding the direct BEM and the indirect BEM, Kirkup⁵ employed these two methods to solve acoustic problems. He also solved the problem of fictitious frequency. These frequencies do not have any physical meaning but are due to the numerical methods. Over five or six decades, many methods were adapted to suppress the fictitious frequency. To overcome this problem, the combined Helmholtz interior integral equation formulation (CHIEF)^{2,6,7} and the Burton and Miller approach¹ are two popular ways in the BEM. The CHIEF method was

developed before the Burton and Miller approach. The Burton and Miller approach¹ was valid for all wave numbers by forming a linear combination of the singular integral equation and its normal derivative with an imaginary number. However, the calculation for the hypersingular integration is required in the Burton and Miller approach. To avoid this computation, an alternative method, CHIEF method, was proposed by Schenck.^{2,6} The CHIEF method adopted the additional constraints by collocating the points in the complementary domain (null-field). Because of the reason for benefit of the Burton and Miller approach and the CHIEF method, some researchers compared those methods or adopted the concept of the CHIEF method.

Marburg⁸ reviewed the mechanism of why a fictitious frequency happened, and compared the CHIEF method, the Burton and Miller approach, and their modification that were employed to suppress the fictitious frequency. Marburg and Amini⁹ compared the Burton and Miller approach and the CHIEF method by considering the case of cat's eye. Achenbach *et al.*¹⁰ employed the off-boundary approach in order to overcome the fictitious frequencies free of singularity. Mathematically speaking, the off-boundary approach originates from the null-field formulation. Many researchers^{11–13} applied the CHIEF method to deal with the problem of fictitious frequencies. Schenck used the CHIEF method, which employed the boundary integral equations by collocating the interior point as an auxiliary condition to make up deficient constraint condition. If the chosen point locates on

^{a)}Also at: Department of Mechanical and Mechatronics Engineering, National Taiwan Ocean University, No. 2, Beining Road, Zhongzheng District, Keelung City 20224, Taiwan, Republic of China. Electronic mail: jtchen@mail.ntou.edu.tw

the nodal line of the associated interior eigenproblem, then the CHIEF method fails. To overcome this disadvantage, Wu and Seybert¹⁴ employed a CHIEF-block method and the weighted residual formulation for acoustic problem. For the water wave problem, Ohmatsu¹⁵ presented a combined integral equation method (CIEM), which is similar to the CHIEF-block method for acoustics by Wu and Seybert. In the CIEM, two additional constraints for one interior point result in an overdetermined system to ensure the removal of irregular frequencies.

An enhanced CHIEF method was also proposed by Lee and Wu.¹⁶ The main concern of the CHIEF method is how the number of interior points is selected and where the positions should be located. Although many experiences in numerical experiments have been provided by researchers, analytically determining the criteria for choosing interior points is not available to our knowledge. Many researchers have studied the CHIEF method, for example, Dokumaci,¹⁷ Chen *et al.*,^{18,19} and Chen and Lee.²⁰ For the indirect BEM or the MFS, a mixed-potential approach was employed to avoid the appearance of fictitious frequency in a similar way of the Burton and Miller approach in the direct BIEM/BEM. Brakhage and Werner²¹ have employed a suitable combination of single-layer and double-layer potentials with the same boundary density on the real boundary. Panich²² employed a similar idea to solve exterior acoustic problems at the same time. Later, Hwang and Chang²³ superimposed the hybrid potential on the retracted boundary.

However, no corresponding approach of the CHIEF method in the direct BEM can be extended to the indirect BEM or the MFS. Since the null-field integral equation cannot be obtained in the indirect BEM or the MFS, it is not straightforward to employ the CHIEF idea for overcoming the problem of fictitious frequency in the indirect BIE or the MFS. This is the main concern of this paper as shown in Table I. In the direct BEM, nonuniqueness problem occurs in the case of a fictitious frequency. However, it may result in the nonexistence problem for the indirect BEM once the boundary condition does not fall in the range of integral operator. Since the MFS is the lump source version of the indirect BEM with auxiliary boundary, nonexistence may also occur. In the indirect BEM or the MFS, two possibilities, nonuniqueness and nonexistence, may occur. Based on Fichera's method, we understand how to add the constraints in Laplace's problem. In Ref. 24, adding the constraint equation can determine the constant term to be zero, so that we have a unique solution.

Recently, the singular value decomposition (SVD) method was developed as an important tool in linear algebra. Chen *et al.*²⁵ used the SVD technique and the self-regularization

technique to construct the bordered matrix for obtaining the inverse matrix, so that we can overcome the problem of the rank-deficiency model. Canning²⁶ used the SVD technique to solve the electromagnetic resonance problem. Juhl¹¹ and Poulin²⁷ combined the CHIEF method with the SVD method to filter out the fictitious frequency. Yang²⁸ employed the self-regularization approach to obtain the corresponding constraint equation by way of the SVD technique. However, this approach may have difficulty in obtaining the field response. Later, Lee *et al.*²⁹ combined the self-regularization method and added extra source points in the indirect BEM and MFS to calculate the field solution in the domain for the fictitious frequency. In this paper, we extend this technique to the double-layer potential formulation and the Neumann-type boundary condition. In addition, we also employ the Fredholm alternative theorem to propose a discriminant that can be adopted to check for infinite solution or no solution. Finally, possible failure source points will be analytically and numerically examined.

II. PROBLEM STATEMENTS

By considering the time-harmonic motion, the governing equation of the 2D exterior acoustic problem is the Helmholtz equation as follows:

$$(\nabla^2 + k^2)u(\mathbf{x}) = 0, \quad \mathbf{x} \in \Omega, \quad (1)$$

where ∇^2 is the Laplace operator, \mathbf{x} is the position vector of the field point, $k = \omega/c$ is the wave number, in which ω is the angular frequency, c is the speed of sound, and Ω is the domain of interest, as shown in Fig. 1.

For simplicity, the soft and hard boundary conditions for the radiator are considered in the following equations.

The soft boundary condition (Dirichlet condition) is

$$u(\mathbf{x}) = \bar{u}(\mathbf{x}), \quad \mathbf{x} \in \partial\Omega, \quad (2)$$

and the hard boundary condition (Neumann condition) is

$$t(\mathbf{x}) = \frac{\partial u(\mathbf{x})}{\partial n_{\mathbf{x}}} = \bar{t}(\mathbf{x}), \quad \mathbf{x} \in \partial\Omega, \quad (3)$$

where $\partial\Omega$ is the boundary of the domain Ω , $n_{\mathbf{x}}$ is the unit outward normal vector of the field point \mathbf{x} , $\bar{u}(\mathbf{x})$ and $\bar{t}(\mathbf{x})$ are boundary data. It is noted that the over-bar symbol in Eqs. (2) and (3) stand for the corresponding density along the boundary.

III. PRESENT APPROACHES

In this section, we adopted two numerical methods of boundary-type. One is the indirect BEM. The other is the

TABLE I. Methods to suppress the appearance of fictitious frequency.

| | Direct BEM | Indirect BEM or MFS | |
|-----------------------------------|---|--|--|
| Burton and Miller method (Ref. 1) | $[ikT + M]\{u\} = [ikU + L]\{t\}$ | $[ikU + T]\{\alpha\} = \{\bar{u}\}$ or $[ikL + M]\{\alpha\} = \{\bar{t}\}$ | Mixed-potential method (Refs. 21 and 22) |
| CHIEF method (Ref. 2) | $\begin{bmatrix} T \\ TC \end{bmatrix} \{u\} = \begin{bmatrix} U \\ UC \end{bmatrix} \{t\}$ | $\begin{bmatrix} U & U_1 \\ \psi_1^H & 0 \end{bmatrix} \begin{Bmatrix} \alpha \\ \beta_1 \end{Bmatrix} = \begin{Bmatrix} \bar{u} \\ 0 \end{Bmatrix}$ | Present approach |

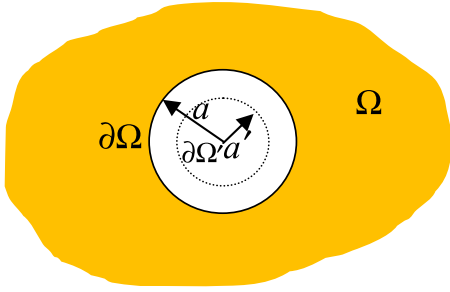


FIG. 1. (Color online) Sketch of the 2D exterior acoustic problem.

MFS. In the present indirect BEM, the source points are distributed along the real boundary. However, these two methods for solving exterior acoustic problems are governed by the Helmholtz equation. We may encounter the problem of fictitious frequencies. It is noted that the problem of fictitious frequency is originating from using the integral equation with the fundamental solution before discretization. Therefore, the problem of zero division by zero due to the fictitious frequency occurs in not only the continuous system (BIE) but also the discrete system (influence matrix). Therefore, the numerical instability may occur when the wave number is equal to the related fictitious frequency.

A. Indirect boundary element method

By using the indirect BEM, the field solution of Eq. (1) can be represented as shown below

$$u(\mathbf{x}) = \int_{\partial\Omega} U(\mathbf{s}, \mathbf{x})\alpha(\mathbf{s})dB(\mathbf{s}), \quad \mathbf{x} \in \Omega, \quad (4)$$

where \mathbf{s} is the position vector of the source point, $U(\mathbf{s}, \mathbf{x})$ is the fundamental solution of the 2D Helmholtz equation, $\alpha(\mathbf{s})$ is the fictitious boundary density and $dB(\mathbf{s})$ is the boundary integral arc length. Here, the adopted fundamental solution is

$$U(\mathbf{s}, \mathbf{x}) = -\frac{i}{4}H_0^{(1)}(kr), \quad (5)$$

where $r \equiv |\mathbf{s} - \mathbf{x}|$ is the distance between the source point and the field point, i is the imaginary number with $i^2 = -1$, $H_0^{(1)}$ is the zeroth-order Hankel function of the first kind and $U(\mathbf{s}, \mathbf{x})$ satisfies the following equation

$$(\nabla^2 + k^2)U(\mathbf{s}, \mathbf{x}) = \delta(\mathbf{x} - \mathbf{s}), \quad (6)$$

in which the $\delta(\mathbf{x} - \mathbf{s})$ denotes the Dirac delta function. It is noted that only the single-layer potential is used in Eq. (4). In addition, we can also employ the double-layer potential to express the field function of Eq. (1) as shown below:

$$u(\mathbf{x}) = \int_{\partial\Omega} T(\mathbf{s}, \mathbf{x})\alpha_D(\mathbf{s})dB(\mathbf{s}), \quad \mathbf{x} \in \Omega, \quad (7)$$

where $T(\mathbf{s}, \mathbf{x})$ and $\alpha_D(\mathbf{s})$ are the double-layer potential and the fictitious boundary density due to $T(\mathbf{s}, \mathbf{x})$, respectively. The definition of $T(\mathbf{s}, \mathbf{x})$ is

$$T(\mathbf{s}, \mathbf{x}) = \frac{\partial U(\mathbf{s}, \mathbf{x})}{\partial n_{\mathbf{s}}}, \quad (8)$$

where $n_{\mathbf{s}}$ is the unit outward normal vector of the source point \mathbf{s} .

To matching the Dirichlet or the Neumann boundary condition by using the single-layer potential approach in Eq. (4), we have

$$\bar{u}(\mathbf{x}) = \int_{\partial\Omega} U(\mathbf{s}, \mathbf{x})\alpha(\mathbf{s})dB(\mathbf{s}), \quad \mathbf{x} \in \partial\Omega, \quad (9)$$

$$\bar{t}(\mathbf{x}) = \int_{\partial\Omega} L(\mathbf{s}, \mathbf{x})\alpha(\mathbf{s})dB(\mathbf{s}), \quad \mathbf{x} \in \partial\Omega, \quad (10)$$

where

$$L(\mathbf{s}, \mathbf{x}) = \frac{\partial U(\mathbf{s}, \mathbf{x})}{\partial n_{\mathbf{x}}} \quad (11)$$

is the normal derivative of $U(\mathbf{s}, \mathbf{x})$ for the field point \mathbf{x} . Similarly, we have following two equations by using the double-layer potential approach in Eq. (7),

$$\bar{u}(\mathbf{x}) = \int_{\partial\Omega} T(\mathbf{s}, \mathbf{x})\alpha_D(\mathbf{s})dB(\mathbf{s}), \quad \mathbf{x} \in \partial\Omega, \quad (12)$$

$$\bar{t}(\mathbf{x}) = \int_{\partial\Omega} M(\mathbf{s}, \mathbf{x})\alpha_D(\mathbf{s})dB(\mathbf{s}), \quad \mathbf{x} \in \partial\Omega, \quad (13)$$

where

$$M(\mathbf{s}, \mathbf{x}) = \frac{\partial T(\mathbf{s}, \mathbf{x})}{\partial n_{\mathbf{x}}} \quad (14)$$

is the normal derivative of $T(\mathbf{s}, \mathbf{x})$ for the field point \mathbf{x} . We employed the constant element scheme to discretize four indirect boundary integral equations in Eqs. (9), (10), (12), and (13) into the discrete system and used the Dirac-Delta collocation as a test function to obtain simultaneous equations. Therefore, we have

$$[U]\{\alpha\} = \{\bar{u}\}, \quad (15)$$

$$[L]\{\alpha\} = \{\bar{t}\}, \quad (16)$$

$$[T]\{\alpha_D\} = \{\bar{u}\}, \quad (17)$$

$$[M]\{\alpha_D\} = \{\bar{t}\}. \quad (18)$$

It is noted that if we solve the above four linear algebraic equations for the special wave number, the inverse matrices of four influence matrices may not be determined. The special wave number is called the fictitious frequency or the spurious resonance frequency in the area of BEM. Owing to those fictitious frequencies, four linear integral operators in Eqs. (9), (10), (12), and (13) are range deficient and four influence matrices are rank deficient. Therefore, the solution of the fictitious boundary densities $\{\alpha\}$ and $\{\alpha_D\}$ are infinite solution or no solution. For the case of no solution, the result of fictitious boundary density is unstable in the numerical implementation. In other words, when the wave number is equal to the fictitious frequency, the certain basis of the field solution cannot be accurately represented by using the indirect BEM in the case

of fictitious frequency. It indicates that the boundary integral equation obtained by using Eq. (4) to match the boundary condition is not sufficient for solving the 2D Helmholtz equation when the wave number is equal to the related fictitious frequency. In addition, it is interesting that the fictitious frequency is the same with eigenvalues of the corresponding interior Dirichlet or Neumann problems.^{5,20}

B. CHIEF idea and self-regularization technique

To deal with the problem of the rank-deficiency due to fictitious frequencies, we employed the self-regularization technique²⁵ to obtain a bordered influence matrix. By using the self-regularization technique for Eq. (15), we employed the technique of singular value decomposition (SVD) to add a slack variable and a constraint equation as shown below:

$$\begin{bmatrix} U & \phi_1 \\ \psi_1^H & 0 \end{bmatrix} \begin{Bmatrix} \alpha_r \\ c_1 \end{Bmatrix} = \begin{Bmatrix} \bar{u} \\ 0 \end{Bmatrix}, \quad (19)$$

where α_r is the column vector of regularized fictitious boundary density, c_1 is a slack variable, the superscript H denotes the operator of Hermitian transpose, ϕ_1 and ψ_1 are the left and right unitary vectors corresponding to the minimum singular value of the influence matrix $[U]$. The SVD structure of the influence matrix $[U]$ is

$$[U]_{N \times N} = [\Phi]_{N \times N} [\Sigma]_{N \times N} [\Psi]_{N \times N}^H, \quad (20)$$

where N is the number of constant elements, the matrix $[\Phi]$ is the left unitary matrix constructed by the left unitary vectors $[\phi_N, \dots, \phi_3, \phi_2, \phi_1]$, $[\Psi]$ is the right unitary matrix constructed by the right unitary vector $[\psi_N, \dots, \psi_3, \psi_2, \psi_1]$ and $[\Sigma]$ is a diagonal matrix as

$$[\Sigma] = \begin{bmatrix} \sigma_N & \cdots & 0 \\ \vdots & \ddots & \vdots \\ 0 & \cdots & \sigma_1 \end{bmatrix}_{N \times N}, \quad (21)$$

in which

$$\sigma_N \geq \cdots \geq \sigma_3 \geq \sigma_2 \geq \sigma_1 \geq 0. \quad (22)$$

It is noted that the influence matrix in Eq. (19) is full rank not only for regular frequencies but also for fictitious frequencies. This influence matrix can also be called as a bordered matrix of $[U]$. However, Eq. (19) is only suitable for the problem of rank-deficiency by 1 due to the fictitious frequency. In the other words, the fictitious frequency is a single root. For the case of rank-deficiency by 2, we added two slack variables and two constraint equations into Eq. (15) as shown below:

$$\begin{bmatrix} U & \phi_1 & \phi_2 \\ \psi_1^H & 0 & 0 \\ \psi_2^H & 0 & 0 \end{bmatrix} \begin{Bmatrix} \alpha_r \\ c_1 \\ c_2 \end{Bmatrix} = \begin{Bmatrix} \bar{u} \\ 0 \\ 0 \end{Bmatrix}. \quad (23)$$

In this way, the influence matrix is invertible for the case of a double root. Although we can obtain a full rank influence

matrix for all wave numbers by using the self-regularization technique, the slack variable cannot represent the field solution inside the domain. After all, the influence matrix $[U]$ in Eq. (15) is just a linear transformation from the fictitious boundary density to the boundary condition. The left unitary vectors and right unitary vectors are the orthogonal bases of the boundary condition and the fictitious boundary density, respectively. This is the reason why the terms $c_1\phi_1$ and $c_2\phi_2$ cannot represent the field solution inside the domain.

In this stage, we have the aid of the CHIEF idea to improve the disadvantage of the self-regularization technique. From the viewpoint of the degenerate kernel, we know that a fundamental solution may contain all bases of the solution space. To represent the deficient basis due to the fictitious frequency, we add some extra source points in the complementary domain. The process of adding extra source points is similar to adding CHIEF points in the direct BEM. In this way, the expression of the field solution in Eq. (4) is improved to

$$u(\mathbf{x}) = \int_{\partial\Omega} U(\mathbf{s}, \mathbf{x})\alpha(\mathbf{s})dB(\mathbf{s}) + \sum_{j=1}^{N_r} \beta_j U(\mathbf{s}_j, \mathbf{x}), \quad \mathbf{x} \in \Omega, \quad (24)$$

where N_r and β_j are the number of the rank-deficiency and the strength of the j th extra source point, respectively. The role of those extra source points can provide deficient bases in the solution embedding the fictitious frequency. On the other hand, all remainder solution bases are expressed from the integral term of Eq. (24). Consequently, we need N_r constraint equations to capture the undetermined parts of the fictitious boundary density $\alpha(\mathbf{s})$. These undetermined parts of $\alpha(\mathbf{s})$ are caused from the fictitious frequency. To achieve our above purpose, we employ the same constraint equations in the self-regularization technique as shown below:

$$\{\psi_j\}^H \{\alpha\} = 0, \quad j = 1, 2, \dots, N_r. \quad (25)$$

We, then, use Eq. (24) to match the Dirichlet-type boundary condition. Then, we have

$$\bar{u}(\mathbf{x}) = \int_{\partial\Omega} U(\mathbf{s}, \mathbf{x})\alpha(\mathbf{s})dB(\mathbf{s}) + \sum_{j=1}^{N_r} \beta_j U(\mathbf{s}_j, \mathbf{x}), \quad \mathbf{x} \in \partial\Omega. \quad (26)$$

After, discretizing Eq. (26), we have

$$[U]\{\alpha\} + \sum_{j=1}^{N_r} \beta_j \{U_j\} = \{\bar{u}\}, \quad (27)$$

where $\{U_j\}$ is the boundary potential of the j th singularity. Combining Eq. (27) with Eq. (25) for the case of a single root, we have

$$\begin{bmatrix} U & U_1 \\ \psi_1^H & 0 \end{bmatrix} \begin{Bmatrix} \alpha \\ \beta_1 \end{Bmatrix} = \begin{Bmatrix} \bar{u} \\ 0 \end{Bmatrix}. \quad (28)$$

It is noted that Eq. (28) is very similar to Eq. (19). The difference between two equations is the source of adding terms.

TABLE II. Comparison between the present approach and the CHIEF method.

| | Present approach | CHIEF method |
|-----------------------------|---|-------------------------------------|
| Extra points | Source points (Fundamental solutions) | Field points (Null-field equations) |
| Role of extra points | Providing deficient bases | Providing constraint equations |
| Extra constraint equations | Need from the SVD | No need anymore |
| Criterion of failure points | Associated nodal lines of the corresponding interior free vibration problem | |

In the self-regularization technique, the adding terms are from its own influence matrix $[U]$. In the present approach, the adding terms are from the extra fundamental solutions. Similarly, we can obtain the following equation for the case of a double root:

$$\begin{bmatrix} U & U_1 & U_2 \\ \psi_1^H & 0 & 0 \\ \psi_2^H & 0 & 0 \end{bmatrix} \begin{Bmatrix} \alpha \\ \beta_1 \\ \beta_2 \end{Bmatrix} = \begin{Bmatrix} \bar{u} \\ 0 \\ 0 \end{Bmatrix}. \quad (29)$$

Although the present approach can provide the deficient bases, there is a risk of selecting position of the extra source points. If an extra source point locates at failure positions, a deficient basis cannot be represented from the extra fundamental solution. The examination of failure

positions is also analogous to the CHIEF method. The comparison between the present approach and the CHIEF method is shown in Table II. In addition, the application of the present idea to the double-layer potential approach and the case of the Neumann boundary condition is stated in the Appendix A.

IV. ANALYTICAL DERIVATION OF POSSIBLE FAILURE POINTS BY USING THE DEGENERATE KERNEL

To derive the possible failure positions of extra source points in the analytical manner, we adopt the circular case and the corresponding degenerate kernel. The closed-form fundamental solution can be expanded to the degenerate kernel by using the polar coordinates as shown below:

$$U(\mathbf{s}, \mathbf{x}) = \begin{cases} \frac{-i}{4} \sum_{m=0}^{\infty} \varepsilon_m J_m(k\rho_s) H_m^{(1)}(k\rho_x) \cos(m(\phi_s - \phi_x)), & \rho_x \geq \rho_s, \\ \frac{-i}{4} \sum_{m=0}^{\infty} \varepsilon_m J_m(k\rho_x) H_m^{(1)}(k\rho_s) \cos(m(\phi_s - \phi_x)), & \rho_x < \rho_s, \end{cases} \quad (30)$$

where the field point \mathbf{x} is expressed as $\mathbf{x} = (\rho_x, \phi_x)$, the source point \mathbf{s} is expressed as $\mathbf{s} = (\rho_s, \phi_s)$ in the polar coordinates, $J_m(\cdot)$ is the m th-order Bessel function of the first kind and ε_m is the Neumann factor as shown below:

$$\varepsilon_m = \begin{cases} 1, & m = 0, \\ 2, & m = 1, 2, \dots, \infty. \end{cases} \quad (31)$$

To fully utilize the orthogonality of triangular functions and the property of the circular boundary, we employ the Fourier series to expand the fictitious boundary density $\alpha(\mathbf{s})$ and the boundary data $\bar{u}(\mathbf{x})$ as shown below:

$$\alpha(\mathbf{s}) = \sum_{n=0}^{\infty} a_n \cos(n\phi_s) + \sum_{n=1}^{\infty} b_n \sin(n\phi_s), \quad \mathbf{s} \in \partial\Omega, \quad (32)$$

$$\bar{u}(\mathbf{x}) = \sum_{n=0}^{\infty} p_n \cos(n\phi_x) + \sum_{n=1}^{\infty} q_n \sin(n\phi_x), \quad \mathbf{x} \in \partial\Omega, \quad (33)$$

where a_n and b_n are the unknown coefficients and p_n and q_n are known constants from the specific boundary data. The boundary integral arc length $dB(\mathbf{s})$ is equal to $\rho_s d\phi_s$ in the

polar coordinates. By substituting Eq. (30), (32), and (33) into Eq. (26), we have

$$\begin{aligned} & \sum_{n=0}^{\infty} p_n \cos(n\phi_x) + \sum_{n=1}^{\infty} q_n \sin(n\phi_x) \\ &= \int_0^{2\pi} \left(\frac{-i}{4} \sum_{m=0}^{\infty} \varepsilon_m J_m(k\rho_s) H_m^{(1)}(k\rho_x) \cos(m(\phi_s - \phi_x)) \right) \\ & \quad \times \left(\sum_{n=0}^{\infty} a_n \cos(n\phi_s) + \sum_{n=1}^{\infty} b_n \sin(n\phi_s) \right) \rho_s d\phi_s \\ & \quad + \sum_{j=1}^{N_r} \beta_j \left(\frac{-i}{4} \sum_{m=0}^{\infty} \varepsilon_m J_m(k\rho_{s_j}) H_m^{(1)}(k\rho_x) \right. \\ & \quad \left. \times \cos(m(\phi_{s_j} - \phi_x)) \right), \\ & \rho_s = \rho_x = a, \end{aligned} \quad (34)$$

where a stands for the radius of the circular boundary. By employing the orthogonal relations of triangular functions for Eq. (34), we have

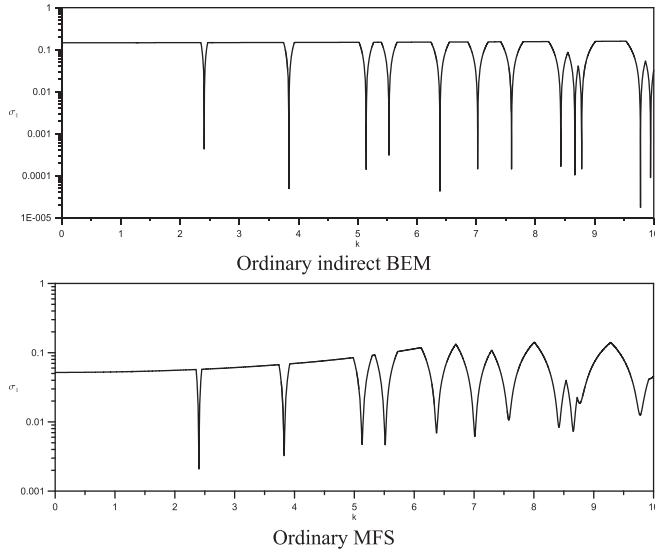


FIG. 2. Spectrum of the minimum singular value σ_1 versus k .

$$\begin{aligned}
 & \sum_{n=0}^{\infty} p_n \cos(n\phi_x) + \sum_{n=1}^{\infty} q_n \sin(n\phi_x) \\
 &= \frac{-\pi i}{2} \sum_{n=0}^{\infty} a_n a J_n(ka) H_n^{(1)}(ka) \cos(n\phi_x) \\
 &+ \frac{-\pi i}{2} \sum_{n=0}^{\infty} b_n a J_n(ka) H_n^{(1)}(ka) \sin(n\phi_x) \\
 &+ \sum_{j=1}^{N_r} \beta_j \left(\frac{-i}{4} \sum_{m=0}^{\infty} \varepsilon_m J_m(k\rho_{s_j}) H_m^{(1)}(ka) \right. \\
 &\quad \left. \times \cos(m(\phi_{s_j} - \phi_x)) \right). \tag{35}
 \end{aligned}$$

By using the orthogonal relations for $\cos(v\phi_x)$ and $\sin(v\phi_x)$, we have

$$\begin{aligned}
 2\pi p_0 &= -\pi^2 i a_0 a J_0(ka) H_0^{(1)}(ka) \\
 &+ \sum_{j=1}^{N_r} \beta_j \left(\frac{-i\pi}{2} \right) J_0(k\rho_{s_j}) H_0^{(1)}(ka), \tag{36} \\
 \pi p_v &= -\frac{\pi^2 i}{2} a_v a J_v(ka) H_v^{(1)}(ka) \\
 &+ \sum_{j=1}^{N_r} \beta_j \left(\frac{-i\pi}{2} \right) J_v(k\rho_{s_j}) H_v^{(1)}(ka) \cos(v\phi_{s_j}), \\
 v &= 1, 2, 3, \dots, \tag{37}
 \end{aligned}$$

TABLE III. The former five fictitious frequencies in the range of $0 < k < 10$ by using the single-layer potential for the Dirichlet boundary condition.

| | k_1 Single root | k_2 Double root | k_3 Double root | k_4 Single root | k_5 Double root |
|----------------------|-------------------|-------------------|-------------------|-------------------|-------------------|
| Indirect BEM | 2.409 | 3.838 | 5.144 | 5.529 | 6.390 |
| MFS | 2.402 | 3.827 | 5.130 | 5.516 | 6.373 |
| $J_n(k \cdot 1) = 0$ | 2.405 | 3.832 | 5.136 | 5.520 | 6.380 |
| | ($n = 0$) | ($n = 1$) | ($n = 2$) | ($n = 0$) | ($n = 3$) |

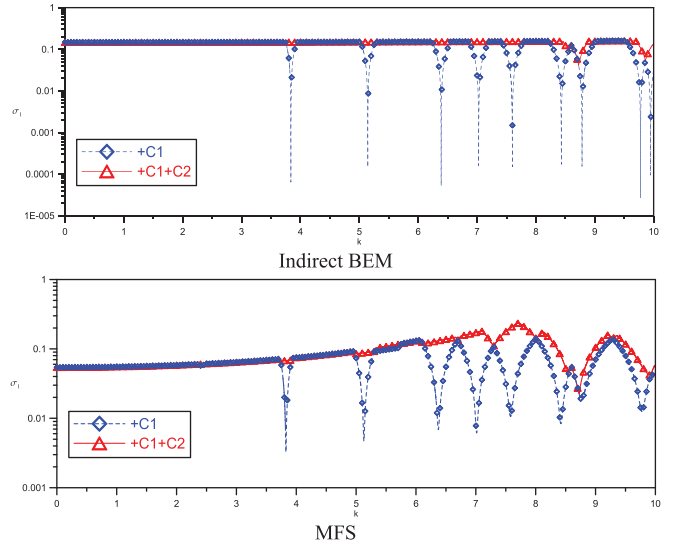


FIG. 3. (Color online) Spectrum of the minimum singular value σ_1 versus k by using the self-regularization technique.

$$\begin{aligned}
 \pi q_v &= -\frac{\pi^2 i}{2} b_v \rho_s J_v(ka) H_v^{(1)}(ka) \\
 &+ \sum_{j=1}^{N_r} \beta_j \left(\frac{-i\pi}{2} \right) J_v(k\rho_{s_j}) H_v^{(1)}(ka) \sin(v\phi_{s_j}), \\
 v &= 1, 2, 3, \dots \tag{38}
 \end{aligned}$$

There are two possible cases in the following derivation. One is the case of rank-deficiency by 1 ($N_r = 1$). The other is the case of rank-deficiency by 2 ($N_r = 2$).

For the first case ($N_r = 1$), the characteristic equation of the fictitious frequency is

$$J_0(k_f a) = 0, \tag{39}$$

where k_f stands for the fictitious frequency. Since we know the right unitary vector corresponding to the zero singular value in the case of $N_r = 1$ is a uniform distribution along the boundary,³⁰ the constraint equation in Eq. (25) can be equivalent to

$$\int_0^{2\pi} \alpha(s) 1 \rho_s d\phi_s = 0. \tag{40}$$

Substituting Eq. (32) to Eq. (40), we have

$$a_0 = 0. \tag{41}$$

Then, substitution of Eq. (41) to Eq. (36), yields

TABLE IV. The former five fictitious frequencies in the range of $0 < k < 10$ by using the double-layer potential for the Dirichlet boundary condition.

| | k_1 Single root | k_2 Double root | k_3 Double root | k_4 Single root | k_5 Double root |
|-----------------------|-------------------|-------------------|-------------------|-------------------|-------------------|
| Indirect BEM | 0.001 | 1.845 | 3.062 | 3.837 | 4.214 |
| MFS | 0.017 | 1.841 | 3.054 | 3.831 | 4.201 |
| $J'_n(k \cdot 1) = 0$ | 0 | 1.841 | 3.054 | 3.832 | 4.201 |
| | ($n = 0$) | ($n = 1$) | ($n = 2$) | ($n = 0$) | ($n = 3$) |

TABLE V. Exact solution of four illustrative examples.

| Case | Exact solution $u(\mathbf{x})$ | Boundary condition $\bar{u}(\mathbf{x})$ | Single-layer potential | Double-layer potential |
|------|--|--|--------------------------|------------------------|
| | | | $k(\text{indirect BEM})$ | |
| | | | $k(\text{MFS})$ | |
| 1 | $\frac{H_0^{(1)}(k\rho_x)}{H_0^{(1)}(ka)}$ | 1 | 2.409 | 3.837 |
| | | | 2.402 | 3.831 |
| 2 | $\frac{H_1^{(1)}(k\rho_x)}{H_1^{(1)}(ka)}\sin(\phi_x)$ | $\sin(\phi_x)$ | 2.409 | 3.837 |
| | | | 2.402 | 3.831 |
| 3 | $\frac{H_0^{(1)}(k\rho_x)}{H_0^{(1)}(ka)}$ | 1 | 3.838 | 1.845 |
| | | | 3.827 | 1.841 |
| 4 | $\frac{H_1^{(1)}(k\rho_x)}{H_1^{(1)}(ka)}\sin(\phi_x)$ | $\sin(\phi_x)$ | 3.838 | 1.845 |
| | | | 3.827 | 1.841 |

$$2\pi p_0 = \beta_1 \left(\frac{-i\pi}{2} \right) J_0(k_f \rho_{s_j}) H_0^{(1)}(k_f a), \quad (42)$$

for the fictitious frequency k_f . This result indicates that the adding fundamental solution can provide the basis corresponding the coefficient p_0 . If the position of the extra source point brings the $J_0(k_f \rho_{s_j})$ term to be zero, the adding fundamental solution may not work. In the other words, the following equation:

$$J_0(k_f \rho_{s_j}) = 0 \quad (43)$$

is the discriminant for the positions of the failure point with respect to the first case. It is interesting that those positions of the failure point are equal to nodal lines of the corresponding interior mode of the circular domain. This finding is the same with the CHIEF method in the direct BEM.¹⁸

Similarly, the characteristic equation of the fictitious frequency for the case of double root ($N_r = 2$) is

$$J_w(k_f a) = 0, \quad w = 1, 2, 3, \dots \quad (44)$$

In this case, the two right unitary vectors corresponding to the zero singular values are $\cos(w\phi_x)$ and $\sin(w\phi_x)$ distributions along the boundary,³⁰ the two constraint equations are equivalent to

$$\int_0^{2\pi} \alpha(\mathbf{s}) \cos(w\phi_x) \rho_s d\phi_s = 0, \quad (45)$$

$$\int_0^{2\pi} \alpha(\mathbf{s}) \sin(w\phi_x) \rho_s d\phi_s = 0. \quad (46)$$

By substituting Eq. (32) into Eq. (45) and (46), we have

$$a_w = 0, \quad (47)$$

$$b_w = 0. \quad (48)$$

According to the results of Eqs. (47) and (48), Eqs. (37) and (38) can be reduced to

$$\pi p_w = \sum_{j=1}^2 \beta_j \left(\frac{-i\pi}{2} \right) J_w(k_f \rho_{s_j}) H_w^{(1)}(k_f a) \cos(w\phi_{s_j}), \quad (49)$$

$$\pi q_w = \sum_{j=1}^2 \beta_j \left(\frac{-i\pi}{2} \right) J_w(k_f \rho_{s_j}) H_w^{(1)}(k_f a) \sin(w\phi_{s_j}), \quad (50)$$

$$\begin{aligned} \pi p_v &= -\frac{\pi^2 i}{2} a_v a J_v(ka) H_v^{(1)}(ka) \\ &+ \sum_{j=1}^{N_r} \beta_j \left(\frac{-i\pi}{2} \right) J_v(k\rho_{s_j}) H_v^{(1)}(ka) \cos(v\phi_{s_j}), \\ v &= 1, 2, 3, \dots, v \neq w, \end{aligned} \quad (51)$$

$$\begin{aligned} \pi q_v &= -\frac{\pi^2 i}{2} b_v a J_v(ka) H_v^{(1)}(ka) \\ &+ \sum_{j=1}^{N_r} \beta_j \left(\frac{-i\pi}{2} \right) J_v(k\rho_{s_j}) H_v^{(1)}(ka) \sin(v\phi_{s_j}), \\ v &= 1, 2, 3, \dots, v \neq w. \end{aligned} \quad (52)$$

Arranging Eqs. (49) and (50), we can obtain the following linear algebraic equation to determine the strengths of the extra source points

$$\begin{aligned} &\left(\frac{-i}{2} \right) H_w^{(1)}(k_f a) \\ &\times \begin{bmatrix} J_w(k_f \rho_{s_1}) \cos(w\phi_{s_1}) & J_w(k_f \rho_{s_2}) \cos(w\phi_{s_2}) \\ J_w(k_f \rho_{s_1}) \sin(w\phi_{s_1}) & J_w(k_f \rho_{s_2}) \sin(w\phi_{s_2}) \end{bmatrix} \\ &\times \begin{Bmatrix} \beta_1 \\ \beta_2 \end{Bmatrix} = \begin{Bmatrix} p_w \\ q_w \end{Bmatrix}. \end{aligned} \quad (53)$$

TABLE VI. The results of the Fredholm alternative theorem by using the indirect BEM.

| Case | Single-layer potential | Double-layer potential |
|------|--|---|
| 1 | No solution | No solution |
| | $\{\phi_1\}^H \{\bar{u}\} = 7.071 + 0.025i$ | $\{\phi_1\}^H \{\bar{u}\} = 2.412 + 6.739i$ |
| 2 | Infinite solution | Infinite solution |
| | $\{\phi_1\}^H \{\bar{u}\} = (4.520 - 1.842i) \cdot 10^{-11}$ | $\{\phi_1\}^H \{\bar{u}\} = (7.201 + 1.616i) \cdot 10^{-11}$ |
| 3 | Infinite solution | Infinite solution |
| | $\{\phi_1\}^H \{\bar{u}\} = (-0.312 + 4.333i) \cdot 10^{-11}$ $\{\phi_2\}^H \{\bar{u}\} = (-0.195 + 2.169i) \cdot 10^{-13}$ | $\{\phi_1\}^H \{\bar{u}\} = (4.037 - 2.465i) \cdot 10^{-11}$ $\{\phi_2\}^H \{\bar{u}\} = (-6.893 + 3.991i) \cdot 10^{-10}$ |
| 4 | No solution | No solution |
| | $\{\phi_1\}^H \{\bar{u}\} = -4.993 + 0.257i$ $\{\phi_2\}^H \{\bar{u}\} = (-1.120 + 0.044i) \cdot 10^{-3}$ | $\{\phi_1\}^H \{\bar{u}\} = (0.529 + 1.056i) \cdot 10^{-3}$ $\{\phi_2\}^H \{\bar{u}\} = -3.536 - 3.535i$ |

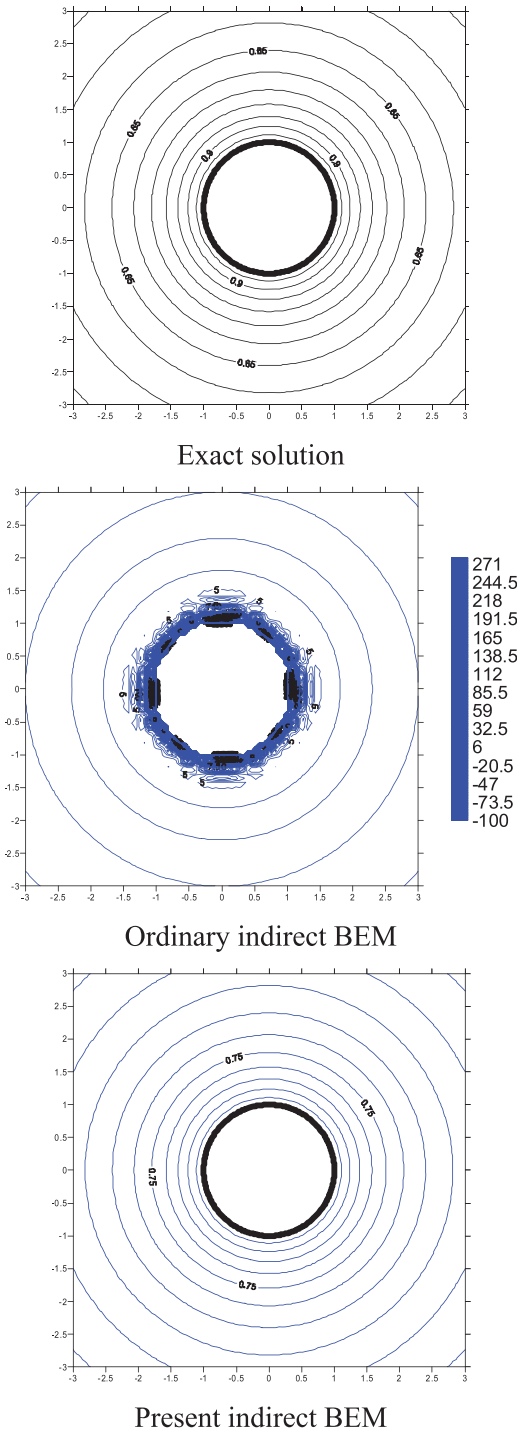


FIG. 4. (Color online) Contour plots of the case 1 by using the indirect BEM with the single-layer potential.

If the positions of the two extra source points bring the determinant of the matrix to be zero,

$$J_w(k_f \rho_{s_1}) J_w(k_f \rho_{s_2}) \sin(w(\phi_{s_2} - \phi_{s_1})) = 0, \quad (54)$$

the strengths (β_1, β_2) of two extra source points cannot be determined. Equation (54) is the discriminant for the positions of the failure point with respect to the case of the double root. This criterion includes two parts,

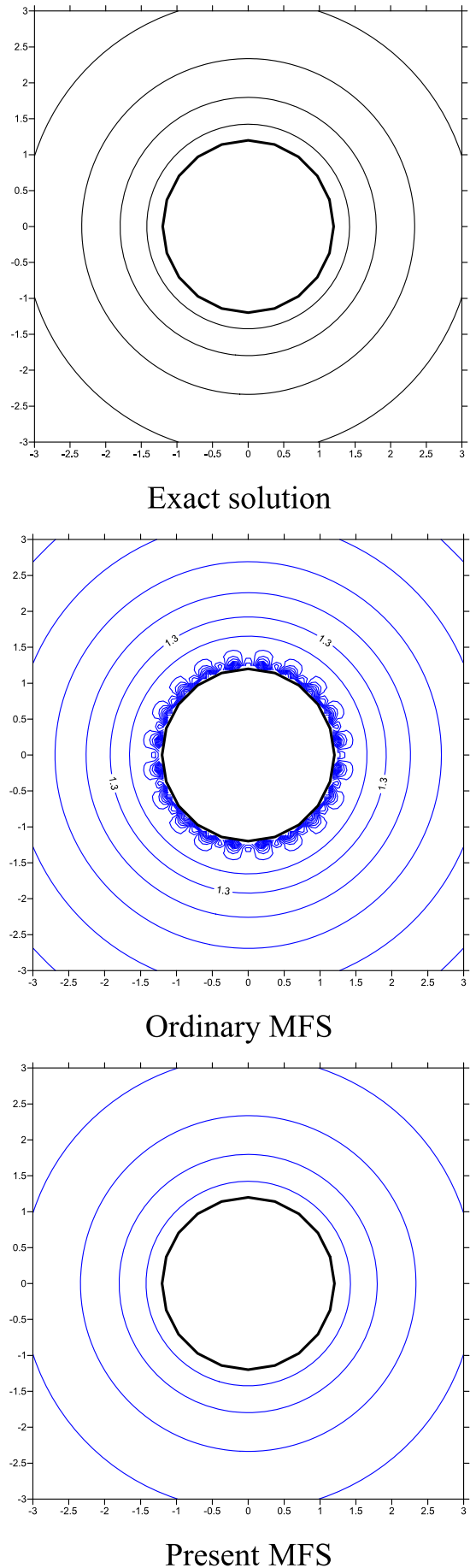
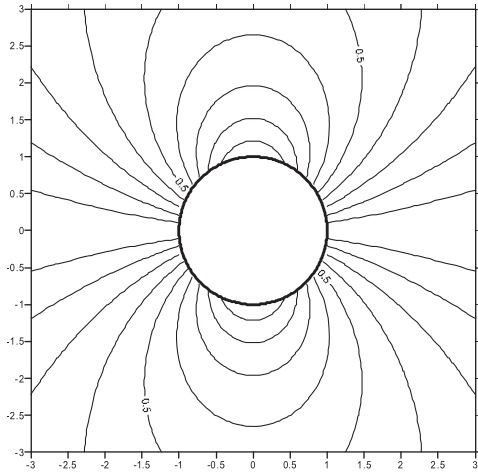
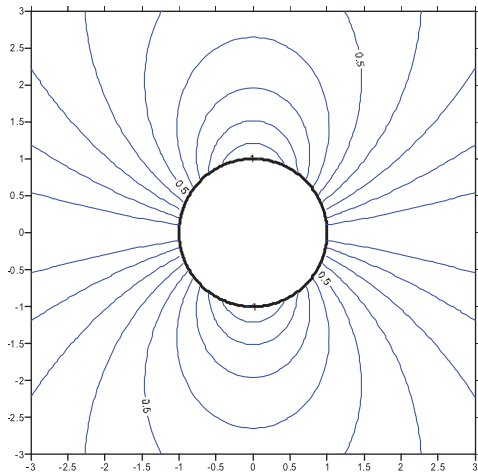


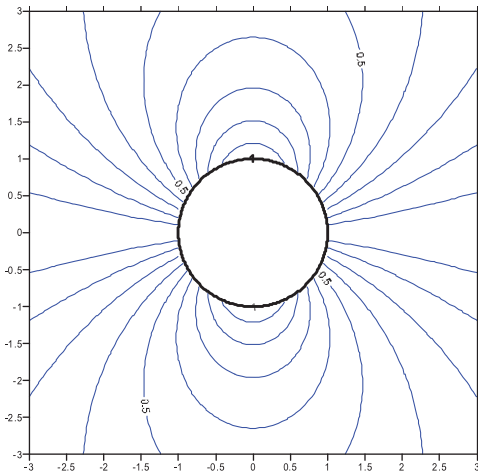
FIG. 5. (Color online) Contour plots of the case 1 by using the MFS.



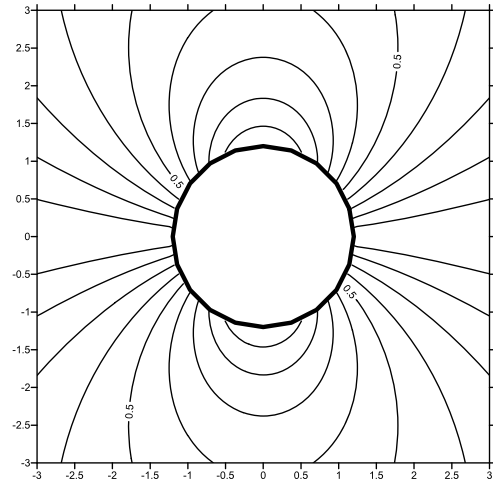
Exact solution



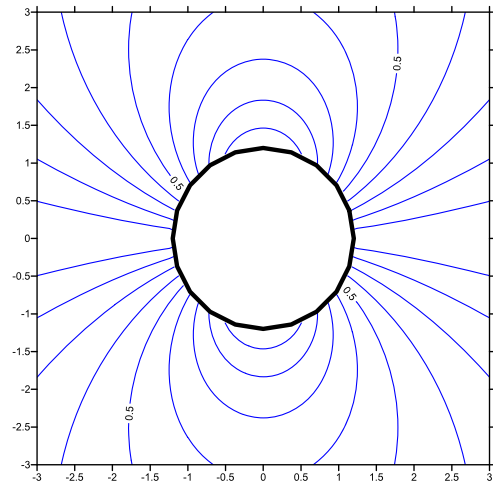
Ordinary indirect BEM



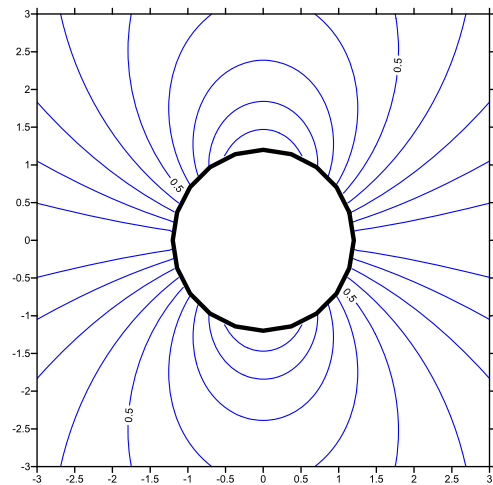
Present indirect BEM



Exact solution



Ordinary MFS



Present MFS

FIG. 6. (Color online) Contour plots of the case 2 by using the indirect BEM with the single-layer potential.

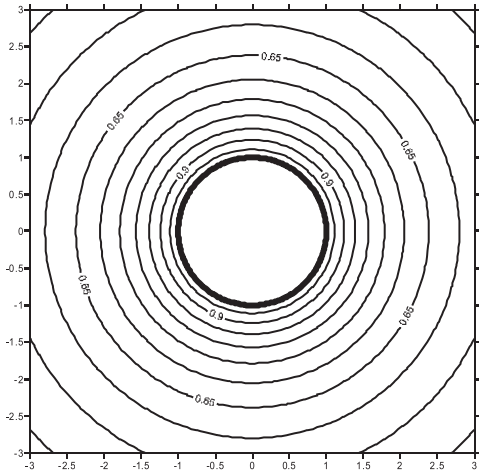
$$J_w(k_f \rho_{s_j}) = 0, \quad j = 1 \text{ or } 2, \quad (55)$$

$$\sin(w\phi) = 0, \quad (56)$$

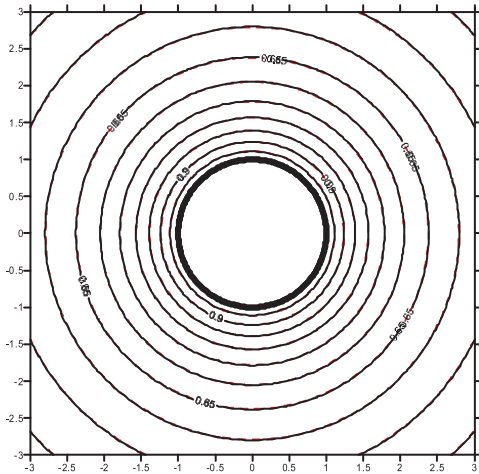
where $\phi = \phi_{s_2} - \phi_{s_1}$ indicates the intersection angle ϕ between the two extra source points.

FIG. 7. (Color online) Contour plots of the case 2 by using the MFS.

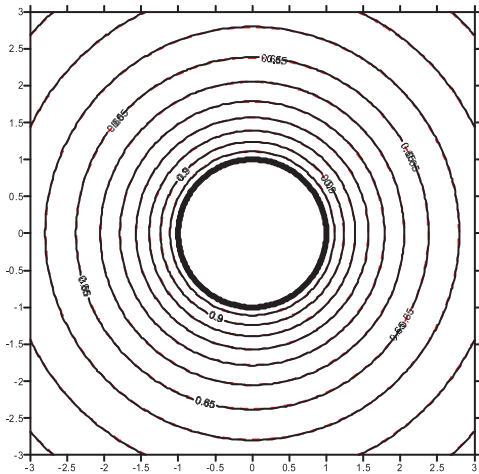
- (1) Equation (55) indicates that if the location of one extra source point satisfies $J_w(k_f \rho_{s_j}) = 0$, the present approach may fail to deal with the problem of fictitious frequencies in the case of the double root.



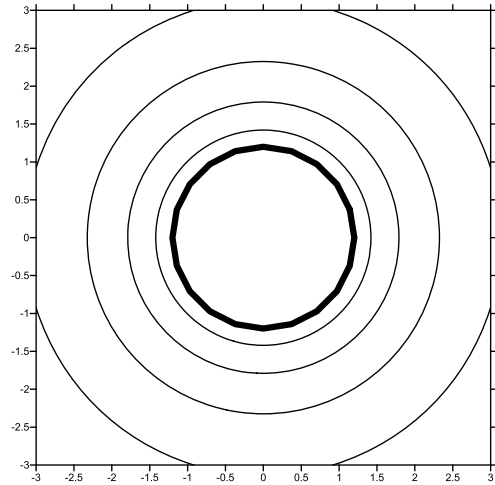
Exact solution



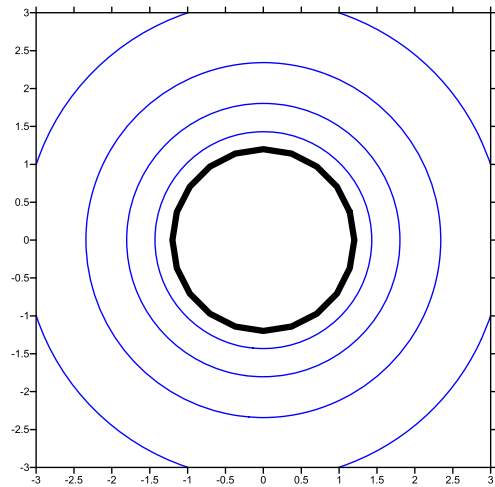
Ordinary indirect BEM



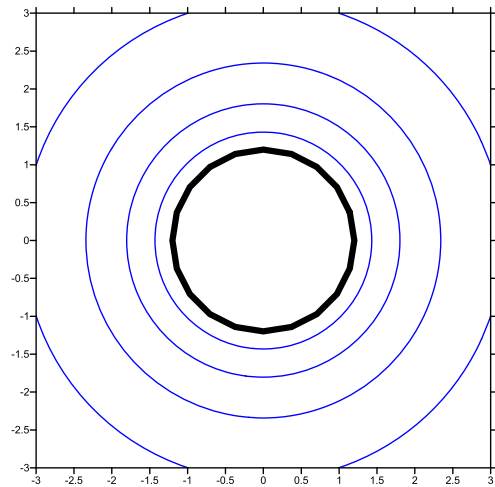
Present indirect BEM



Exact solution



Ordinary MFS



Present MFS

FIG. 8. (Color online) Contour plots of the case 3 by using the indirect BEM with the single-layer potential.

(2) Equation (56) indicates that if the intersection angle ϕ equals to π/w , the determinant of the matrix may also be zero in the case of the double root.

The above two results are also the same with the results of the CHIEF method in the direct BEM. This is the reason

FIG. 9. (Color online) Contour plots of the case 3 by using the MFS.

why the present approach is similar to the CHIEF method.¹⁸ Therefore, the present approach can fill in the blank area that there is no CHIEF method in the indirect BEM as shown in Table I.

V. METHOD OF FUNDAMENTAL SOLUTIONS IN CONJUNCTION WITH THE CHIEF IDEA AND THE SELF-REGULARIZATION TECHNIQUE

The MFS can be seen as a discrete version of the indirect BIEM by considering the lump source. The problem of numerical instability due to fictitious frequencies may encounter in using the MFS to solve the 2D exterior acoustic problem. The acoustic field can be expressed by using the MFS as shown below:

$$u(\mathbf{x}) = \sum_{i=1}^N \gamma_i U(\mathbf{s}_i, \mathbf{x}), \quad \mathbf{s}_i \in \partial\Omega', \quad (57)$$

where γ_i is the strength of the i th source point, N is the number of source points and $\partial\Omega'$ is a fictitious boundary outside the domain. In the MFS, the source points are located on the fictitious boundary. $U(\mathbf{s}_i, \mathbf{x})$ is the fundamental solution of the 2D Helmholtz equation as shown in Eq. (5). To obtain simultaneous equations, we select N collocation points \mathbf{x} on the boundary by matching the Dirichlet boundary condition to have

$$\{\bar{u}\} = [U]\{\gamma\}. \quad (58)$$

However, the influence matrix is singular in Eq. (58) for a fictitious frequency. Similarly, we also introduce the CHIEF idea and the self-regularization technique to overcome the rank-deficiency problem due to fictitious frequencies.

Similarly, we add some extra source points in Eq. (57) to provide the solution basis for the range-deficiency problem caused by the fictitious frequency as shown below:

$$u(\mathbf{x}) = \sum_{i=1}^N \gamma_i U(\mathbf{s}_i, \mathbf{x}) + \sum_{j=1}^{N_r} \beta_j U(\mathbf{s}_j, \mathbf{x}),$$

$$\mathbf{s}_i \in \partial\Omega', \quad \mathbf{s}_j \notin \partial\Omega'. \quad (59)$$

It is noted that the extra source points cannot be located on the fictitious boundary. We collocated N field points and employed Eq. (59) to satisfy the boundary condition to obtain the following equation:

$$[U]\{\gamma\} + \sum_{j=1}^{N_r} \beta_j \{U_j\} = \{\bar{u}\}. \quad (60)$$

Next, the corresponding constraint equations are obtained from the singular value decomposition of the influence matrix in Eq. (58) as shown below:

$$\{\psi_j\}^H \{\gamma\} = 0, \quad j = 1, 2, \dots, N_r. \quad (61)$$

By combining Eq. (60) with Eq. (61) for the case of single root ($N_r = 1$) and the case of double roots ($N_r = 2$), we have the same form of linear algebraic equations as Eq. (28) and Eq. (29).

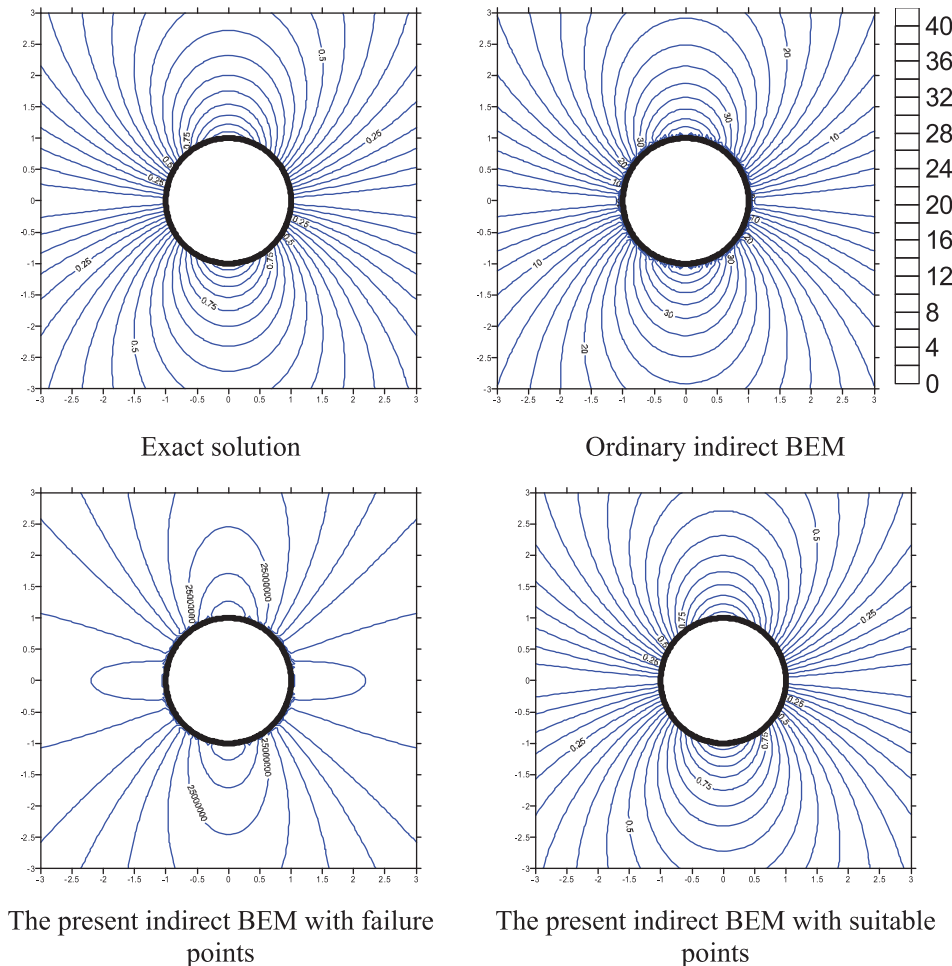


FIG. 10. (Color online) Contour plots of the case 4 by using the indirect BEM with the single-layer potential.

For $N_r = 1$, we have

$$\begin{bmatrix} U & U_1 \\ \psi_1^H & 0 \end{bmatrix} \begin{Bmatrix} \gamma \\ \beta_1 \end{Bmatrix} = \begin{Bmatrix} \bar{u} \\ 0 \end{Bmatrix}. \quad (62)$$

For $N_r = 2$, we have

$$\begin{bmatrix} U & U_1 & U_2 \\ \psi_1^H & 0 & 0 \\ \psi_2^H & 0 & 0 \end{bmatrix} \begin{Bmatrix} \gamma \\ \beta_1 \\ \beta_2 \end{Bmatrix} = \begin{Bmatrix} \bar{u} \\ 0 \\ 0 \end{Bmatrix}. \quad (63)$$

In addition, the discriminant for the positions of the failure point is the same with that of Sec. IV.

VI. NUMERICAL EXAMPLES

First, we demonstrate the validity of the self-regularization technique in the indirect BEM and the MFS. The 2D exterior acoustic problem containing circular radiator is considered as shown in Fig. 1. In using the indirect BEM, the radius of the radiator is $a = 1$. In using the MFS, the radii of the radiator and the fictitious boundary are $a = 1.2$ and $a' = 1$, respectively. We adopted 50 constant elements and 20 source points in the indirect BEM and the MFS, respectively. Figure 2 shows the spectrums of the minimum singular value by using the ordinary indirect BEM

[Eq. (15)] and the ordinary MFS [Eq. (58)]. It is found that fictitious frequencies happen to be k -value at drops. The former five fictitious frequencies in the range of $0 < k < 10$ are listed in Table III. It is found that values of fictitious frequencies are very close to zeros of Bessel function of the first kind. When we only employed the self-regularization technique to construct the bordered (influence) matrices, the minimum singular value is not equal to zero any more as shown in Fig. 3. Although the influence matrices are invertible, the field solution inside the domain cannot be determined. We not only employ the single-layer potential formulation but also the double-layer potential formulation. Similarly, the former five fictitious frequencies in the range of $0 < k < 10$ are listed in Table IV. From the results of Tables III and IV, it is obvious that fictitious frequencies depend on kernel functions we used. Next, we consider four examples with the Dirichlet boundary condition to check the validity of combining the CHIEF idea with the self-regularization technique for determining the field solution. The exact solutions and adopted fictitious frequencies are summarized in Table V. Furthermore, the way to discriminate the case of no solution or infinite solution is summarized in Appendix B. According to the results of the Fredholm alternative theorem as shown in Table VI, it is found that the cases 1 and 4 are the cases of no solution. On the contrary, the cases 2 and 3 are the cases of infinite solution.

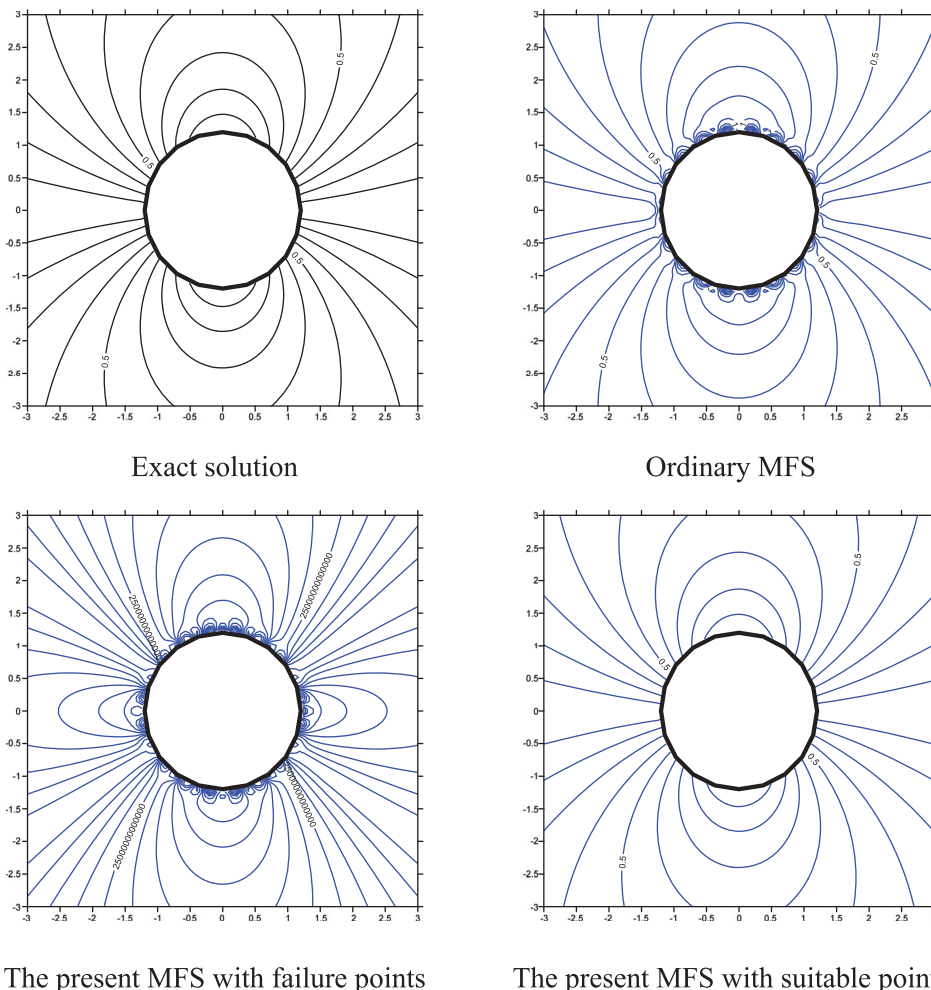


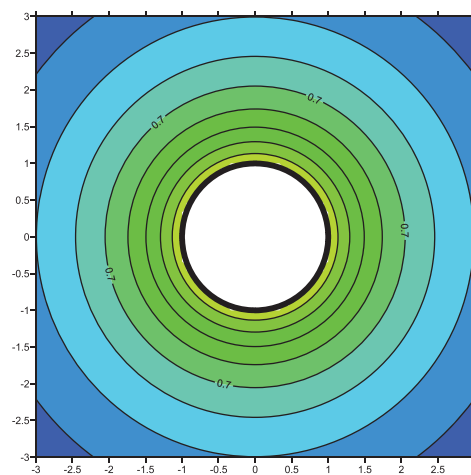
FIG. 11. (Color online) Contour plots of the case 4 by using the MFS.

In the case 1, the contour plots of potential by using the exact solution and the ordinary indirect BEM are shown in Fig. 4. It is obvious that the numerical result obtained from the ordinary indirect BEM is incorrect. Therefore, we employ the present approach with an extra source point $\mathbf{s}_1 = (0, 0)$ to determine the appropriate field solution as shown in Fig. 4. The position of this extra source point does not fall in satisfying Eq. (43) and consequently is not a failure point. In other words, the extra source point $\mathbf{s}_1 = (0, 0)$ can provide the deficient basis caused by the fictitious frequency $k_f = 2.409$. Similarly, we employed the MFS to solve the case 1 with $k_f = 2.402$, the exact solution is shown in Fig. 5. The incorrect contour plot and the appropriate contour plot by using the ordinary MFS and the present MFS are shown in Fig. 5. Therefore, the present idea with $\mathbf{s}_1 = (0, 0)$ can also effectively deal with the problem of fictitious frequencies.

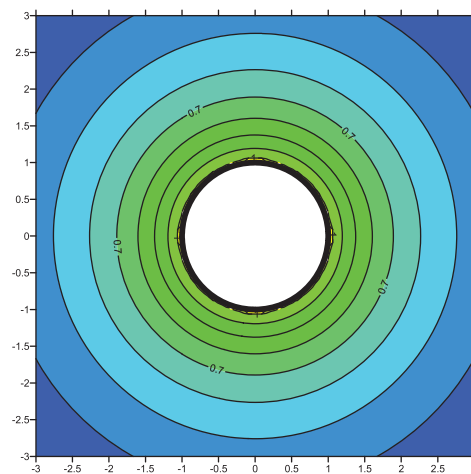
In the cases 2 and 3, all contour plots by using the indirect BEM and the MFS are shown in Figs. 6–9. It is interesting that even though we do not employ the CHIEF idea and the self-regularization technique, we can calculate the appropriate solutions. This phenomenon can be explained by using the Fredholm alternative theorem. These two cases are the situations of infinite solution. The values of slack variables are close to zero in the real implementation. It indicates that although the adopted wave numbers are equal to fictitious frequencies, the corresponding field solutions do not contain the corresponding deficient bases. Therefore, the appropriate solutions can be obtained without using the CHIEF idea and the self-regularization technique. Nevertheless, we can also employ the present regularized approach to obtain the appropriate solutions. An extra source point is $\mathbf{s}_1 = (0, 0)$ for the case 2. Two extra source points are $\mathbf{s}_1 = (0.5, 0)$ and $\mathbf{s}_2 = (0.1, 0.2)$ for the case 3.

In the case 4, the contour plots by using the exact solution and the ordinary indirect BEM are shown in Fig. 10. If the two extra source points are not properly located, e.g., $\mathbf{s}_1 = (-0.5, 0)$ and $\mathbf{s}_2 = (0.5, 0)$, the result of the contour plot is not accurate as shown in Fig. 10. The adopted wave number is close to the first zero of $J_1(k \cdot 1)$ and the intersection angle ϕ between these two extra source points is equal to π . Therefore, the intersection satisfies the discriminant of Eq. (56). This is the reason why the layout of $\mathbf{s}_1 = (-0.5, 0)$ and $\mathbf{s}_2 = (0.5, 0)$ is improper. Nevertheless, by employing two valid locations, $\mathbf{s}_1 = (-0.5, 0)$ and $\mathbf{s}_2 = (0.1, 0.2)$, the new result agrees well with the exact solution as shown in Fig. 10. Those results of the MFS also support the above point as shown in Fig. 11. From the view point of the Fredholm alternative theorem, the cases 1 and 4 have no solution in using the ordinary indirect BEM and the MFS. Therefore, the present approach can play an important role in these two cases.

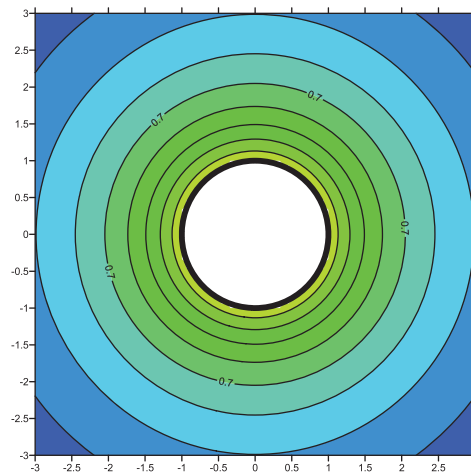
By using the indirect BEM with the double-layer potential, all contour plots are shown in Figs. 12–15. All corresponding extra source points are the same with the extra source points adopted in the single-layer potential. According to Figs. 13 and 14, these two cases are the case of infinite solution. Even though we do not employ the present idea, we still obtain the accurate solutions. For the results of



Exact solution



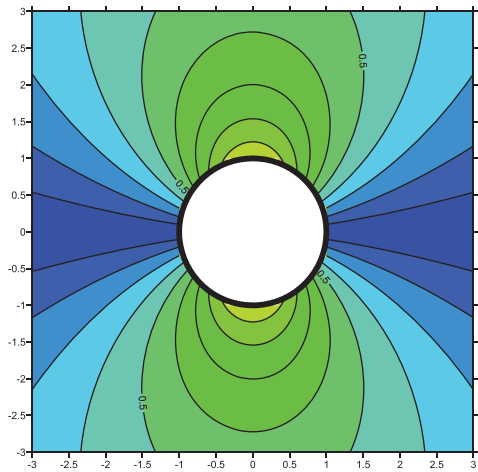
Ordinary indirect BEM



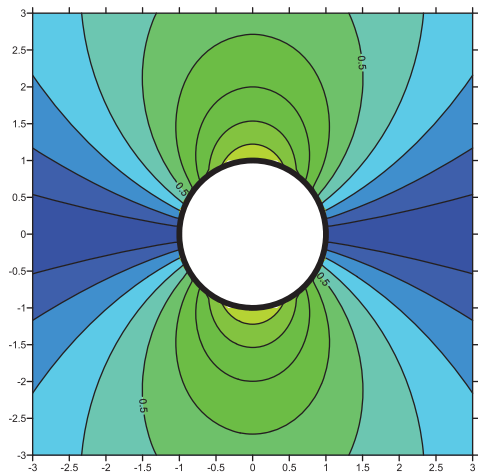
Present indirect BEM

FIG. 12. (Color online) Contour plots of the case 1 by using the indirect BEM with the double-layer potential.

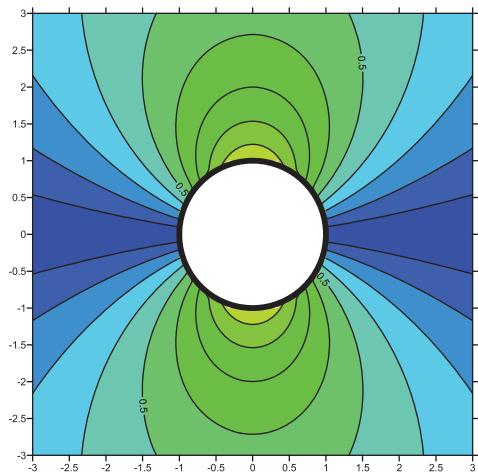
cases 1 and 4 as shown in Figs. 12 and 15, respectively, the accurate results can be determined by adopting present idea with suitable extra source points. Once we collocate the extra source points at the failure position, we may obtain the inaccurate results as shown in Fig. 15.



Exact solution



Ordinary indirect BEM

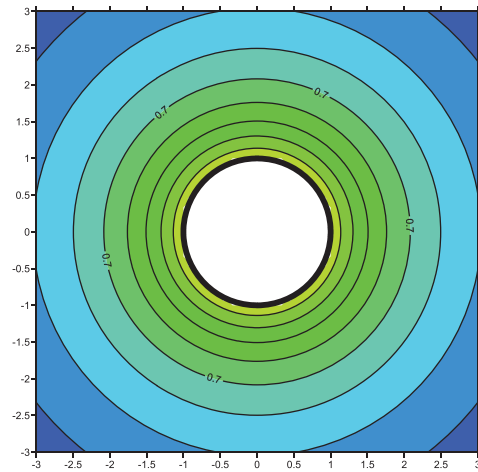


Present indirect BEM

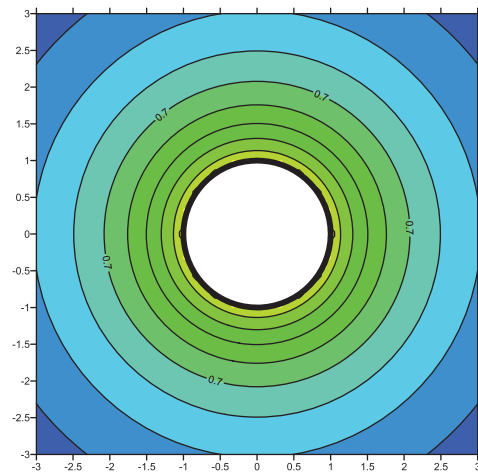
FIG. 13. (Color online) Contour plots of the case 2 by using the indirect BEM with the double-layer potential.

VII. CONCLUSIONS

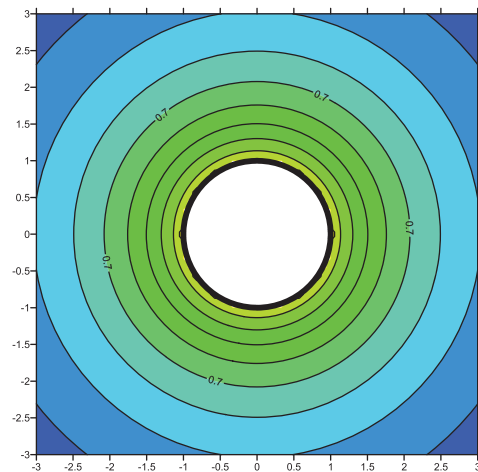
In this paper, we employed the indirect BEM and the MFS in conjunction with the self-regularization technique and the CHIEF idea to deal with the problem of fictitious



Exact solution



Ordinary indirect BEM



Present indirect BEM

FIG. 14. (Color online) Contour plots of the case 3 by using the indirect BEM with the double-layer potential.

frequencies in the 2D exterior Helmholtz problems. Although the bordered matrix obtained by only using the self-regularization technique is invertible for any wave number, the field solution inside the domain still cannot be determined.

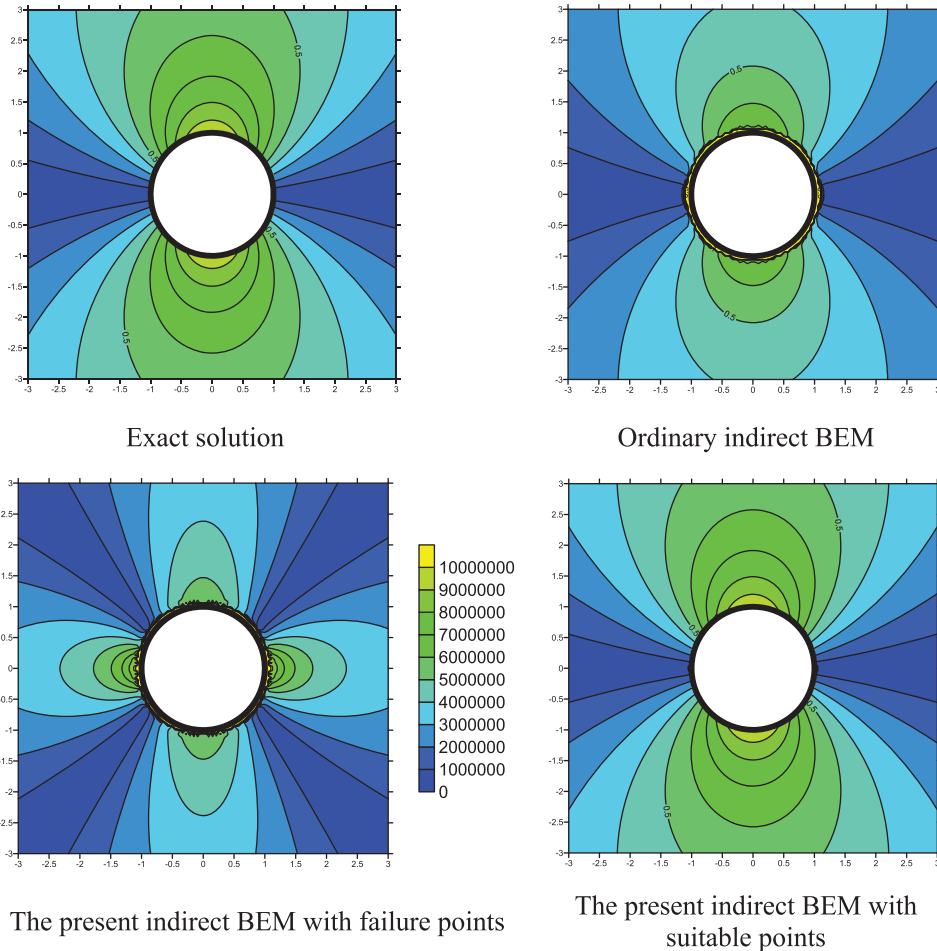


FIG. 15. (Color online) Contour plots of the case 4 by using the indirect BEM with the double-layer potential.

To solve this problem, the extra source points are needed. This idea is very similar to the CHIEF method in the direct BEM since they have the same discriminant of the failure points. Those positions of failure points are associated with nodal lines of the corresponding interior problem. This is the reason why the present approach can fill in the blank area that there is no CHIEF method in the indirect BEM. In using the indirect BEM and the MFS, the problem of fictitious frequencies can be dealt with by adding extra fundamental solutions and adopting constraint equations from the SVD. Finally, four examples were given to verify the validity of the present approach.

ACKNOWLEDGMENT

Financial support from the Ministry of Science and Technology under Grant No. MOST-107-2221-E-019-022 for National Taiwan Ocean University is gratefully acknowledged.

APPENDIX A: DOUBLE-LAYER FORMULATIONS OF THE PRESENT IDEA

According to the experience of applying the present idea to the single-layer potential approach, the double-layer potential approach can be improved as

$$u(\mathbf{x}) = \int_{\partial\Omega} T(\mathbf{s}, \mathbf{x})\alpha_D(\mathbf{s})dB(\mathbf{s}) + \sum_{j=1}^{N_r} \beta_j U(\mathbf{s}_j, \mathbf{x}), \quad \mathbf{x} \in \Omega. \quad (\text{A1})$$

After satisfying the Dirichlet-type boundary condition, we have

$$\bar{u}(\mathbf{x}) = \int_{\partial\Omega} T(\mathbf{s}, \mathbf{x})\alpha_D(\mathbf{s})dB(\mathbf{s}) + \sum_{j=1}^{N_r} \beta_j U(\mathbf{s}_j, \mathbf{x}), \quad \mathbf{x} \in \partial\Omega. \quad (\text{A2})$$

Discretizing Eq. (A2), we have

$$[T]\{\alpha_D\} + \sum_{j=1}^{N_r} \beta_j \{U_j\} = \{\bar{u}\}. \quad (\text{A3})$$

By using the self-regularization technique, the corresponding constraint equation is

$$\{\psi_{Tj}\}^H \{\alpha_D\} = 0, \quad j = 1, 2, \dots, N_r, \quad (\text{A4})$$

where $\{\psi_{Tj}\}$ denotes the right unitary vector corresponding the j th zero singular value of the influence matrix $[T]$. Combining Eq. (A3) with Eq. (A4) for the case of a single root ($N_r = 1$), we have

$$\begin{bmatrix} T & U_1 \\ \psi_{T1}^H & 0 \end{bmatrix} \begin{Bmatrix} \alpha_D \\ \beta_1 \end{Bmatrix} = \begin{Bmatrix} \bar{u} \\ 0 \end{Bmatrix}. \quad (\text{A5})$$

For the case of a double root ($N_r = 2$), we have

$$\begin{bmatrix} T & U_1 & U_2 \\ \psi_{T1}^H & 0 & 0 \\ \psi_{T2}^H & 0 & 0 \end{bmatrix} \begin{Bmatrix} \alpha_D \\ \beta_1 \\ \beta_2 \end{Bmatrix} = \begin{Bmatrix} \bar{u} \\ 0 \\ 0 \end{Bmatrix}. \quad (\text{A6})$$

By using the present idea to matching the Neumann-type boundary condition, we have

$$\bar{t}(\mathbf{x}) = \int_{\partial\Omega} L(\mathbf{s}, \mathbf{x}) \alpha(\mathbf{s}) dB(\mathbf{s}) + \sum_{j=1}^{N_r} \beta_j L(\mathbf{s}_j, \mathbf{x}), \quad \mathbf{x} \in \partial\Omega, \quad (\text{A7})$$

and

$$\bar{t}(\mathbf{x}) = \int_{\partial\Omega} M(\mathbf{s}, \mathbf{x}) \alpha_D(\mathbf{s}) dB(\mathbf{s}) + \sum_{j=1}^{N_r} \beta_j L(\mathbf{s}_j, \mathbf{x}), \quad \mathbf{x} \in \partial\Omega, \quad (\text{A8})$$

by using the single-layer approach and double-layer approach, respectively. The corresponding constraint equations are

$$\{\psi_{L_j}\}^H \{\alpha\} = 0, \quad j = 1, 2, \dots, N_r, \quad (\text{A9})$$

$$\{\psi_{M_j}\}^H \{\alpha_D\} = 0, \quad j = 1, 2, \dots, N_r, \quad (\text{A10})$$

where $\{\psi_{L_j}\}$ and $\{\psi_{M_j}\}$ denote the right unitary vector corresponding the j th zero singular value of the influence matrices $[L]$ and $[M]$, respectively. The finally linear algebraic equations for the case of a single root ($N_r = 1$) are

$$\begin{bmatrix} L & L_1 \\ \psi_{L1}^H & 0 \end{bmatrix} \begin{Bmatrix} \alpha \\ \beta_1 \end{Bmatrix} = \begin{Bmatrix} \bar{t} \\ 0 \end{Bmatrix}, \quad (\text{A11})$$

$$\begin{bmatrix} M & L_1 \\ \psi_{M1}^H & 0 \end{bmatrix} \begin{Bmatrix} \alpha_D \\ \beta_1 \end{Bmatrix} = \begin{Bmatrix} \bar{t} \\ 0 \end{Bmatrix}. \quad (\text{A12})$$

For the case of a double root ($N_r = 2$), we have

$$\begin{bmatrix} L & L_1 & L_2 \\ \psi_{L1}^H & 0 & 0 \\ \psi_{L2}^H & 0 & 0 \end{bmatrix} \begin{Bmatrix} \alpha \\ \beta_1 \\ \beta_2 \end{Bmatrix} = \begin{Bmatrix} \bar{t} \\ 0 \\ 0 \end{Bmatrix}, \quad (\text{A13})$$

$$\begin{bmatrix} M & L_1 & L_2 \\ \psi_{M1}^H & 0 & 0 \\ \psi_{M2}^H & 0 & 0 \end{bmatrix} \begin{Bmatrix} \alpha_D \\ \beta_1 \\ \beta_2 \end{Bmatrix} = \begin{Bmatrix} \bar{t} \\ 0 \\ 0 \end{Bmatrix}. \quad (\text{A14})$$

In addition, the same criterion [Eqs. (43), (55), and (56)] for the positions of the failure point can be analytically derived by using the degenerate kernels.

APPENDIX B: FREDHOLM ALTERNATIVE THEOREM

According to the Fredholm alternative theorem, if the following linear algebra equation

$$[U]\{\alpha\} = \{\bar{u}\} \quad (\text{B1})$$

has a unique solution, the influence matrix $[U]$ is nonsingular. Conversely, if the influence matrix $[U]$ is singular there are two situations for the solution $\{\alpha\}$. One is no solution. The other is infinite solution. By using the SVD, we can discriminate the case of no solution or infinite solution. For the case of a single root ($N_r = 1$), we have

$$[U]^H \{\phi_1\} = \{0\}, \quad (\text{B2})$$

where $\{\phi_1\}$ is the left unitary vector corresponding the zero singular value. By left multiplying Eq. (B1) by $\{\phi_1\}^H$, yields

$$\{\phi_1\}^H [U] \{\alpha\} = \{\phi_1\}^H \{\bar{u}\}. \quad (\text{B3})$$

By substituting Eq. (B2) to Eq. (B3), we have

$$\{\phi_1\}^H \{\bar{u}\} = \{0\}^H \{\alpha\}. \quad (\text{B4})$$

According to the result of Eq. (B4), there are two possible situations. If the term $\{\phi_1\}^H \{\bar{u}\}$ is not equal to zero, the solution $\{\alpha\}$ is no solution. On the other hand, the solution $\{\alpha\}$ is infinite solution when the term $\{\phi_1\}^H \{\bar{u}\}$ is equal to zero.

For the case of a double root ($N_r = 2$), we have

$$[U]^H \{\phi_i\} = \{0\}, \quad i = 1, 2. \quad (\text{B5})$$

Similarly, we left multiply Eq. (B1) by $\{\phi_1\}^H$ and $\{\phi_2\}^H$, which yields

$$\{\phi_i\}^H [U] \{\alpha\} = \{\phi_i\}^H \{\bar{u}\}, \quad i = 1, 2. \quad (\text{B6})$$

By substituting Eq. (B5) to Eq. (B6), we have

$$\{\phi_i\}^H \{\bar{u}\} = \{0\}^H \{\alpha\}, \quad i = 1, 2. \quad (\text{B7})$$

Finally, the same result can be obtained. If one of them $\{\phi_i\}^H \{\bar{u}\}$ is not equal to zero, the solution $\{\alpha\}$ is no solution. On the other hand, the solution $\{\alpha\}$ is infinite solution when the two terms $\{\phi_1\}^H \{\bar{u}\}$ and $\{\phi_2\}^H \{\bar{u}\}$ are equal to zero.

¹A. J. Burton and G. F. Miller, "The application of integral equation methods to numerical solutions of some exterior boundary value problem," *Proc. R. Soc. A* **323**, 201–210 (1971).

²H. A. Schenck, "Improved integral formulation for acoustic radiation problems," *J. Acoust. Soc. Am.* **44**, 41–58 (1968).

³J. T. Chen, L. W. Liu, and H.-K. Hong, "Spurious and true eigensolutions of Helmholtz BIEs and BEMs for a multiply-connected problem," *Proc. R. Soc. A* **459**, 1891–1924 (2003).

⁴I. L. Chen, "Using the method of fundamental solutions in conjunction with the degenerate kernel in cylindrical acoustic problems," *J. Chin. Inst. Eng.* **29**, 445–457 (2011).

⁵S. Kirkup, *The Boundary Element Method in Acoustics* (Integrated Sound Software, Heptonstall, UK, 1998).

⁶H. A. Schenck, "Helmholtz integral formulation of the sonar equations," *J. Acoust. Soc. Am.* **79**, 1423–1433 (1986).

⁷W. Benthien and A. Schenck, "Nonexistence and non-uniqueness problems associated with integral equation method in acoustics," *Comput. Struct.* **65**, 295–305 (1997).

⁸S. Marburg and B. Nolte, *Computational Acoustics of Noise Propagation in Fluids—Finite and Boundary Element Methods* (Springer, Berlin, 2008).

- ⁹S. Marburg and S. Amini, "Cat's eye radiation with boundary elements: Comparative study on treatment of irregular frequencies," *J. Comput. Acoust.* **13**, 21–45 (2005).
- ¹⁰J. D. Achenbach, G. E. Kechter, and Y.-L. Xu, "Off-boundary approach to the boundary element method," *Comput. Methods Appl. Mech. Eng.* **70**, 191–201 (1988).
- ¹¹P. Juhl, "A numerical study of the coefficient matrix of the boundary element method near characteristic frequencies," *J. Sound Vib.* **175**, 39–50 (1994).
- ¹²W. Schroeder and I. Wolff, "The origin of spurious modes in numerical solutions of electromagnetic field eigenvalue problems," *IEEE Trans. Microwave Theory Tech.* **42**, 644–653 (1994).
- ¹³A. F. Seybert and T. K. Rengarajan, "The use of CHIEF to obtain unique solutions for acoustic radiation using boundary integral equations," *J. Acoust. Soc. Am.* **81**, 1299–1306 (1987).
- ¹⁴T. W. Wu and A. F. Seybert, "A weighted residual formulation for the CHIEF method in acoustics," *J. Acoust. Soc. Am.* **90**, 1608–1614 (1991).
- ¹⁵S. Ohmatsu, "A new simple method to eliminate the irregular frequencies in the theory of water wave radiation problems," Papers of Ship Research Institute (1983).
- ¹⁶L. Lee and T. W. Wu, "An enhanced CHIEF method for steady-state elastodynamics," *Eng. Anal. Boundary Elem.* **12**, 75–83 (1993).
- ¹⁷E. Dokumaci, "A study of the failure of numerical solutions in boundary element analysis of acoustic radiation problems," *J. Sound Vib.* **139**, 83–97 (1990).
- ¹⁸I. L. Chen, J. T. Chen, and M. T. Liang, "Analytical study and numerical experiments for radiation and scattering problems using the CHIEF method," *J. Sound Vib.* **248**, 809–828 (2001).
- ¹⁹I. L. Chen, J. T. Chen, S. R. Kuo, and M. T. Liang, "A new method for true and spurious eigensolutions of arbitrary cavities using the CHEEF method," *J. Acoust. Soc. Am.* **109**, 982–999 (2001).
- ²⁰J. T. Chen and J. W. Lee, "Water wave problems using null-field boundary integral equations: Ill-posedness and remedies," *Appl. Anal.* **91**, 675–702 (2012).
- ²¹H. Brakhage and P. Werner, "Über das Dirichletsche aussenraumproblem für die Helmholtzsche schwingungsgleichung" ("About the Dirichlet outer space problem for the Helmholtz equation of oscillation"), *Arch. Math.* **16**, 325–329 (1965).
- ²²O. I. Panich, "On the question of the solvability of the exterior boundary problem for the wave equation and Maxwell's equation," *Usp. Mat. Nauk* **20**, 221–226 (1965), available at <https://reurl.cc/9y0oX>.
- ²³J. Y. Hwang and S. C. Chang, "A retracted boundary integral equation for exterior acoustic problem with unique solution for all wave numbers," *J. Acoust. Soc. Am.* **90**, 1167–1180 (1991).
- ²⁴J. T. Chen, H. Han, S. R. Kuo, and S. K. Kao, "Regularization method for ill-conditioned system of the integral equation of the first kind with the logarithmic kernel," *Inverse Probl. Sci. Eng.* **22**, 1176–1195 (2014).
- ²⁵J. T. Chen, W. S. Huang, J. W. Lee, and Y. C. Tu, "A self-regularized approach for deriving the free-free flexibility and stiffness matrices," *Comput. Struct.* **145**, 12–22 (2014).
- ²⁶F. X. Canning, "Singular value decomposition of integral equation of EM and applications to the cavity resonance problem," *IEEE Trans. Antennas Propag.* **37**, 1156–1163 (1989).
- ²⁷S. Poulin, "A boundary element model for diffraction of water waves on varying water depth," Ph.D. dissertation, Technical University of Denmark, Lyngby (1997).
- ²⁸J. L. Yang, "Rank-deficiency for problem of degenerate scale and fictitious frequencies," Master's thesis, National Taiwan Ocean University, Keelung, Taiwan (2017).
- ²⁹J. W. Lee, C. F. Nien, and J. T. Chen, "Combination of the CHIEF and the self-regularization technique for solving 2D exterior Helmholtz equations with fictitious frequencies in the indirect BEM and MFS," in *Symposium of the International Association for Boundary Element Methods (IABEM 2018)*, Paris, France (2018).
- ³⁰J. T. Chen, J. W. Lee., I. L. Chen, and P. S. Kuo, "On the null and nonzero fields for true and spurious eigenvalues of annular and confocal elliptical membranes," *Eng. Anal. Boundary Elem.* **37**, 42–59. (2013).